

# Contribution of exciton-electron scattering to photoluminescence spectra in semiconductor quantum-wells

H. Ouerdane

*Physics, School of Engineering and Physical Sciences,  
Heriot-Watt University, Edinburgh EH14 4AS, UK and  
Laboratoire CRISMAT, UMR CNRS-ENSICAEN(ISMRA) 6508,  
6 boulevard Maréchal Juin, 14050 Caen Cedex, France*

M. E. Portnoi

*International Center for Condensed Matter Physics,  
Universidade de Brasília, 70919-970 Brasília-DF, Brazil and  
School of Physics, University of Exeter, Exeter EX4 4QL, UK*

I. Galbraith

*Physics, School of Engineering and Physical Sciences,  
Heriot-Watt University, Edinburgh EH14 4AS, UK*

A model that allows direct quantitative comparison between exciton-electron scattering (XES) and electron-hole plasma (EHP) contributions to photoluminescence (PL) in semiconductor quantum-wells (QWs) at room temperature in a low density regime, is presented. We study and compare the XES contribution to PL spectra for mid-gap and wide-gap materials. The balance between the exciton and the free carrier populations is discussed in terms of ionization degree in the non-degenerate regime. The application of the variable phase method yields an expression of the excitonic wavefunctions in a two-dimensional Coulomb potential statically screened by the free carrier gas, that we use to calculate the  $1s$  exciton-free electron scattering matrix elements. The XES and EHP contributions to PL for both ZnSe-based and GaAs-based QWs at room temperature are computed from Fermi's golden rule. In the high temperature and low density regime we find the exciton-electron scattering contribution to PL spectra in ZnSe QW significant whereas it is largely dominated by electron-hole recombination in GaAs QW.

PACS numbers: 71.35.-y, 78.55.-m, 78.55.Cr, 78.55.Et, 78.67.De

## I. INTRODUCTION

Many aspects of photoluminescence in semiconductor quantum-wells have been extensively studied both theoretically and experimentally [1, 2, 3, 4, 5, 6, 7, 8, 9, 10, 11, 12]. PL spectra are indeed useful to study a rich variety of phenomena in semiconductor physics and allow non-destructive characterization of semiconductors. In this paper we are interested in the theoretical study of PL and propose to calculate the related spontaneous emission rates (SER) in the case of a low density mixed exciton/electron-hole plasma in quasi-equilibrium at room temperature. We address specifically the quantitative comparison of exciton-electron scattering and electron-hole plasma contributions to photoluminescence.

Early works by Kubo, Martin and Schwinger [1, 2] suggest that in quasi-equilibrium the intensity of PL is proportional to the absorption coefficient times the Bose distribution describing the photon gas interacting with the semiconductor medium. Detailed studies of the excitonic resonance features and their dynamics through PL spectra based on the KMS approach led to interpret the build-up of the excitonic resonance below the gap as direct evidence of excitonic formation on the sub-nanosecond timescale, see e.g. Refs. [5, 8, 9]. However,

calculations by Kira *et al* [10, 11] clearly show that there is no straightforward connection between exciton formation and the presence of an excitonic peak in the emission. Moreover Chatterjee *et al* [12] have identified conditions under which the PL emission at the exciton resonance after excitation in the continuum is dominated by the free electron-hole plasma or by an incoherent exciton population. Work in Ref. [12] was carried out to study the low temperature regime and they could not determine experimentally the fraction of excitons contributing to PL. Recently, Szczytko *et al* [13] showed that excitons provide the dominant contribution to the luminescence signals at the exciton energy. They conclude that for densities, temperatures, and time scales actually used in time-resolved experiments the Coulomb correlated plasma contribution might be neglected. This clearly gives support to models that take into account the existence of a finite population of excitons in excited QWs, such as the one presented in this article.

In wide-gap materials the bare exciton binding energy,  $E_b^X$ , is of the same order as the thermal energy  $k_B T$  at room temperature because of the greater strength of the Coulomb force;  $E_b^X$  is even larger in QW structures where Coulomb forces are enhanced because of the confinement. Bound exciton states can be observed at high temperature and it has long been known that they play a ma-

ajor role in the optical properties of wide-gap materials [14, 15, 16, 17]. Therefore the inclusion of a finite population of bound exciton states in the calculation of the SER in wide-gap QWs is needed. A complete treatment of the balance between bound excitonic states and free carriers is a difficult problem that has attracted attention for several years [18, 19, 20, 21, 22, 23]. In the case of QWs, advances were made in Ref. [22] where the degree of ionization,  $\alpha$ , of a non-degenerate two-dimensional (2D) electron-hole plasma was calculated. The degree of ionization,  $\alpha$ , whose values are between 0 and 1, gives the proportion of free carriers in the electron-hole plasma. It is defined as the ratio  $N^0/N$  of the density of free carriers,  $N^0$ , to the total plasma density,  $N = N^0 + N^{\text{corr}}$  where  $N^{\text{corr}}$  is the density of Coulomb correlated carriers [19]. The degree of ionization is both density and temperature dependent. Authors of Ref. [22] demonstrated that for wide-gap semiconductor quantum-wells at room temperature, the equilibrium consists of an almost equal mixture of correlated electron-hole pairs and uncorrelated free carriers. This is not the case for mid-gap materials and here we expect this qualitative difference to appear in SER computed from Fermi's golden rule [14, 24, 25].

In this paper, as in Ref. [22], we are mostly interested in the plasma properties induced by the pair Coulomb interaction between charged particles. The plasma temperature being set to  $T = 300$  K, we assume its density to be small enough (non-degenerate limit) to neglect phase-space filling effects. In these conditions, the contribution of Coulomb correlations to PL spectra is the scattering between thermalized  $1s$  excitons with a finite center of mass momentum and free electrons. This assumption is valid at room temperature and moderate densities where the  $1s$  exciton population dominates all other Coulomb correlations in the electron-hole plasma. Moreover in the non-degenerate limit, the scattering of  $1s$  excitons with free electrons is the most likely process contributing to photoluminescence [26] below the band-edge: an exciton leaves its initial state and reach the photon line before radiative recombination, transferring its momentum to its scattering partner, a free electron. Because of heavier mass exciton-hole scattering yields no significant contribution, and we also checked that because of the thermodynamic regime we choose, direct exciton recombination may be safely neglected in the present work. We find that the fraction of excitons that are in the radiative cone and hence can directly recombine, is four orders of magnitude smaller than the total exciton density; and we also performed test calculations that show that in these conditions PL spectra obtained from direct exciton recombination are two orders of magnitude smaller than PL spectra from exciton-electron scattering.

Scattering processes involving excitons are still the object of intensive work. Usually regarded as bosons, Combescot *et al* [27] recently showed that bosonization of excitons is not appropriate to treat the exciton-exciton scattering problem as it yields incorrect scattering rates and lifetime. In this paper we are only con-

cerned with exciton-electron scattering. Calculations in an unscreened Coulomb potential with hydrogen atom-like exciton wavefunctions have been proposed by Kavokin *et al* [28]. In the present work, the electron-hole bound states are computed assuming a statically screened Coulomb potential whose asymptotic behaviour permits the application of the variable phase method [29].

In Section 2 we detail the basic assumptions made for the model of the interacting 2D electron-hole plasma, define the ionization degree and present the formulas of the SER that will be used for this work. Section 3 is devoted to the derivation of the exciton wavefunctions from the variable phase theory. In Section 4 we calculate the exciton-electron scattering matrix elements and derive an expression for the exciton contribution to the spontaneous emission rate. Numerical results are presented and discussed in Section 5, where ZnSe and GaAs QWs PL spectra are compared.

## II. INGREDIENTS FOR THE MODEL

### A. Underlying assumptions

In this work we assume the quantum-well structures to be ideal two-dimensional systems in a two-band model with parabolic dispersion, neglecting detail related to valence-band mixing. We consider a neutral low density, 2D plasma composed of interacting electrons and holes, at room temperature. We thereby remain in the Boltzmann regime neglecting Pauli blocking. The non-degenerate limit is defined by [30]:

$$N\lambda_{m_c}^2/g \ll 1, \quad (1)$$

where  $N$  is the 2D carrier density,  $\lambda_{m_c} = (2\pi\hbar^2/m_c k_B T)^{1/2}$  the thermal wavelength and  $g$  the spin degeneracy of the confined carriers of effective mass  $m_c$ . For  $T = 300$  K, Eq. (1) is satisfied for  $N \ll 1.7 \times 10^{12}$  cm $^2$  for ZnSe-based QWs and  $N \ll 7.2 \times 10^{11}$  cm $^2$  for GaAs-based QWs [22].

Due to spatial confinement of the carriers in QWs the Coulombic interaction between electrons and holes is enhanced. However, even at moderate plasma densities carrier-carrier interactions are weakened because of the density-dependent screening. Screening is one of the most important manifestations of the complex many-body interaction in the electron-hole plasma and the simplest approach is the use of the 2D statically screened potential [31]:

$$V_s(\rho) = \frac{e^2}{\epsilon} \int_0^\infty \frac{q J_0(q\rho)}{q + q_s} dq, \quad (2)$$

where  $J_0$  is the Bessel function;  $q_s$ , in the Boltzmann limit, is known as the 2D Debye-Hückel screening wavenumber (which depends on temperature and carrier

density),  $\epsilon$  is the static dielectric constant of the semiconductor and  $\rho$  the inter-carrier distance. Equation (2) describes the electron-electron and hole-hole repulsion; the attractive electron-hole potential is obtained by changing the overall sign.

The above integral may also be written in terms of special functions:

$$V_s(\rho) = \frac{e^2}{\epsilon} \left[ \frac{1}{\rho} - \frac{\pi}{2} (\mathbf{H}_0(q_s \rho) - N_0(q_s \rho)) \right], \quad (3)$$

where  $N_0$  and  $\mathbf{H}_0$  are the Neumann and Struve functions respectively [32, 33].

The total screening is the sum of electron and hole plasma screenings. As such we neglect the weak screening by neutral excitons.

### B. The degree of ionization

In QWs where Coulomb forces are enhanced because of the spatial confinement of the electrons and holes, we expect a finite population of Coulomb correlated quasi-particles in the plasma even at room temperature. The balance between those correlations and the free carriers is obtained by calculating the degree of ionization,  $\alpha$  [22]:

$$\alpha = \frac{N_a^0}{N_a} = \frac{N_a^0}{N_a^0 + N_a^{\text{corr}}}, \quad (4)$$

where the index  $a$  denotes electron,  $a=e$ , or holes,  $a=h$ .  $N_a^0$ , is the density of uncorrelated particles with renormalized energies. This term is independent of the inter-particle interaction.  $N_a^{\text{corr}}$ , contains all correlation effects both in the bound and continuum states. The densities  $N_a^0$  and  $N_a^{\text{corr}}$  contribute to the total density of a carrier of type  $a$  [19]:

$$N_a = N_a^0 + N_a^{\text{corr}}. \quad (5)$$

When  $\alpha$  is close to unity, the thermodynamic properties of the electron-hole plasma are those of the ideal gas (defined by  $\alpha = 1$ ). For lower values of the degree of ionization the thermodynamic properties of the plasma deviate from those of the ideal gas and Coulomb correlations have to be considered.

Further discussion and detailed calculations on the degree of ionization and the statistical mechanics of the 2D electron-hole plasma can be found in Refs. [22, 34]. Here we only stress that the degree of ionization is obtained from the calculation of the partition function of the 2D electron-hole plasma. Scattering state contributions to the partition function have to be considered in addition to the bound-state sum as a proper account of scattering eliminates singularities in thermodynamic properties of the non-ideal 2D gas caused by the emergence of additional bound states as the strength of the attractive

potential is increased. Inclusion of the scattering states also leads to a strong deviation from the standard law of mass action.

The ionization degrees,  $\alpha_{\text{GaAs}}$  and  $\alpha_{\text{ZnSe}}$ , are shown as a function of plasma density  $N$  on Fig. 1 for GaAs and ZnSe quantum-wells at temperature  $T = 300$  K.  $\alpha_{\text{GaAs}}(N)$  is a monotonic function of  $N$  whereas  $\alpha_{\text{ZnSe}}(N)$  exhibits a minimum at low density. The presence of the minimum is due to the influence of Coulomb screening on the density dependence of the ionization degree: at very low density screening is negligible and  $N_a^{\text{corr}}$  is proportional to the square of the total plasma density so  $\alpha$  is a decreasing function of  $N$ ; however with  $N$  increasing further, plasma screening becomes more and more important and hence reduces the strength of Coulomb correlations so  $N_a^{\text{corr}}$  is a decreasing function of  $N$  and  $\alpha$  increases. This density dependence is more dramatic in ZnSe QWs where Coulomb forces are much stronger than they are in GaAs QWs. Note that  $\alpha_{\text{GaAs}}(N)$  and  $\alpha_{\text{ZnSe}}(N)$  not only differ qualitatively but also quantitatively: in GaAs QWs the electron-hole plasma is dominated by free carriers whereas it contains comparable densities of correlations and free carriers in ZnSe QWs. Knowledge of the degree of ionization is of great importance as the emission mechanisms depend on the nature of the plasma. For further detail see Ref. [22].

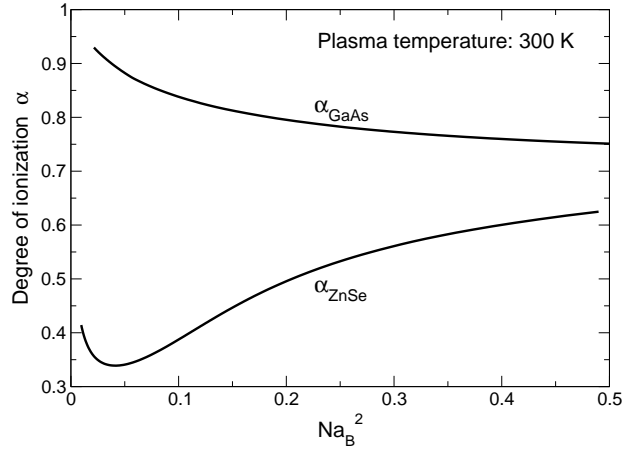


FIG. 1: Ionization degree evaluated for GaAs and ZnSe quantum wells in the Boltzmann regime for  $T = 300$  K, as a function of the 2D plasma density scaled to the square of the excitonic Bohr radius,  $a_B$ .

### C. The spontaneous emission rate

At room temperature a rich variety of scattering processes occur in the exciton/electron-hole plasma, such as exciton-exciton scattering, phonon-exciton scattering, free carrier-exciton scattering, free carrier-phonon scattering. The scattering of  $1s$  excitons with free electrons is considered as one of the dominant mechanisms producing photoluminescence below the band edge at room temper-

ature [26]. In this section we give the general expressions of the electron-hole plasma and exciton-electron scattering contributions to the spontaneous emission rate,  $R_{\text{sp}}^{\text{eh}}(\hbar\Omega)$  and  $R_{\text{sp}}^{\text{corr}}(\hbar\Omega)$ .

The spontaneous emission rate in semiconductors in which the carriers in the conduction band,  $c$ , and the valence band,  $v$ , are both in quasi-equilibrium as characterized by their chemical potentials may be expressed as follows [24]:

$$R_{\text{sp}}^{\text{eh}}(\hbar\Omega) = 2 \sum_{\mathbf{k}} \frac{f_c(E_c(\mathbf{k}))(1 - f_v(E_v(\mathbf{k})))}{\tau_{\text{rad}}} \delta(E_c - E_v - \hbar\Omega), \quad (6)$$

where  $\hbar\Omega$ , the photon energy,  $\tau_{\text{rad}}$  the radiative lifetime and  $f_c(E_c(\mathbf{k}))$  and  $f_v(E_v(\mathbf{k}))$  the distribution function of the carriers within the conduction and valence bands. The sum  $\sum_{\mathbf{k}}$  is performed over the Brillouin zone and the  $\delta$ -function ensures the conservation of energy in the process.

In the Boltzmann limit we find that Eq. (6) may be rewritten as:

$$R_{\text{sp}}^{\text{eh}}(\hbar\Omega) = \frac{2}{\pi} z_e z_h \times \int_0^{\infty} \frac{1}{\tau_{\text{rad}}} \frac{\eta \exp(-\beta E)}{(E_g + E - \hbar\Omega)^2 + \eta^2} dE, \quad (7)$$

where  $m_r$  is the electron-hole reduced mass,  $E_g$  the gap energy, and the homogeneous broadening in the spectrum modelled using a Lorentzian function instead of the  $\delta$ -function in Eq. (6), as  $\lim_{\eta \rightarrow 0} \eta/(x^2 + \eta^2) = \pi\delta(x)$ . The fugacities  $z_a$  appearing in Eq. (7) are calculated in the low density limit:

$$z_a = e^{\beta\mu_a} \approx 1 - \sqrt{1 - \lambda_{m_a}^2 \alpha(N_a) N_a}, \quad (8)$$

where  $\beta$  the inverse thermal energy and  $\mu_a$  is the chemical potential of the carrier gas of type a. Note that  $\tau_{\text{rad}}$  is a function of the photon energy [24]:

$$\tau_{\text{rad}}(\hbar\Omega) = \frac{3\pi c^3 \hbar^4 \epsilon_0}{e^2 n_{\text{op}}(\hbar\Omega)^3 x_{vc}^2}, \quad (9)$$

where  $c$  is the speed of light in the vacuum,  $n_{\text{op}}$  is the optical index of the material and  $x_{vc}$  is the Coulomb enhanced dipole matrix element that characterizes the strength of the dipole transition between the conduction and valence bands. The attractive Coulomb interaction not only generates bound exciton states below the energy gap but also influences significantly the optical properties of the EHP at the band edge and above where absorption and emission spectra are enhanced. This Coulomb enhancement is obtained from the Sommerfeld factor which is proportional to  $|\psi_E(\rho = 0)|^2$ , where  $\psi_E(\rho)$  is the wavefunction of the unbound electron-hole pair with positive energy  $E$ . Calculations of both bound exciton and scattering wavefunctions are presented in the next section.

The expression for  $R_{\text{sp}}^{\text{corr}}(\hbar\Omega)$  is taken from Refs. [14, 25]:

$$R_{\text{sp}}^{\text{corr}}(\hbar\Omega) = \sum_{\mathbf{k}_{\text{cm}}} \sum_{\mathbf{k}_2} C_{\mathbf{k}_{\text{cm}}, \mathbf{k}_2} N_{\mathbf{k}_{\text{cm}}} N_{\mathbf{k}_2}, \quad (10)$$

with

$$C_{\mathbf{k}_{\text{cm}}, \mathbf{k}_2} = \frac{2\pi}{\hbar} |V_{\text{scat}}(k_{\text{cm}})|^2 \left( \frac{4\pi\beta_1\Omega/\omega_0}{(1 - \Omega^2/\omega_0^2)^2 + 4\pi\beta_1} \right) \times \delta \left( E_{\text{X}} - \hbar\Omega - \frac{\hbar^2}{2m_e} (k_{\text{cm}}^2 + 2\mathbf{k}_{\text{cm}} \cdot \mathbf{k}_2) \right), \quad (11)$$

where  $V_{\text{scat}}$  is the exciton - electron scattering matrix element,  $\mathbf{k}_{\text{cm}}$  the exciton center of mass wavevector, and  $\mathbf{k}_2$  the free electron wavevector. The exciton and free carrier distributions,  $N_{\mathbf{k}_{\text{cm}}}$  and  $N_{\mathbf{k}_2}$ , are:

$$N_{\mathbf{k}_{\text{cm}}} = \frac{2\pi\beta\hbar^2}{M} (1 - \alpha) N \exp \left( -\beta \frac{\hbar^2 k_{\text{cm}}^2}{2M} \right), \quad (12)$$

and

$$N_{\mathbf{k}_2} = \frac{2\pi\beta\hbar^2}{m_e} \alpha N \exp \left( -\beta \frac{\hbar^2 k_2^2}{2m_e} \right). \quad (13)$$

The coefficient  $\beta_1$  in Eq. (11) ensures that there is no divergence when the photon energy  $\hbar\Omega$  is equal to the gap energy  $E_g$ . The exciton binding energy is  $E_{\text{b}}^{\text{X}}$ , so the total energy of an exciton is:  $E_{\text{X}} = E_g - E_{\text{b}}^{\text{X}} + \hbar^2 k_{\text{cm}}^2 / 2M$ , with  $M = m_e + m_h$ . For ease of notation in the subsequent calculations we denote  $F(\Omega)$  the factor located between  $|V_{\text{scat}}(k_{\text{cm}})|^2$  and the  $\delta$ -function in Eq. (11).

### III. THE 2D EXCITON WAVEFUNCTION

#### A. Exciton bound states

In this section we calculate the wavefunction of an electron-hole bound state in the statically screened potential, Eq. 2. We suppose that the interaction between the two particles depends only on the relative distance  $\rho = \|\mathbf{r}_e - \mathbf{r}_h\|$ , and we split the problem into two parts: the study of the relative motion of the two particles and the study of the motion of the center of mass which does not depend on the interaction. The total Hamiltonian can then be written as:  $\hat{H}_{\text{tot}} = \hat{H}_{\text{cm}} + \hat{H}_{\text{rel}}$ . To study the relative motion problem we apply the variable phase method of scattering theory, neglecting the intrinsic spin effects.

The Schrödinger equation for the radial wavefunction of the relative motion has the following form:

$$\left[ \frac{d^2}{d\rho^2} + \frac{1}{\rho} \frac{d}{d\rho} + \kappa^2 - U(\rho) - \frac{m^2}{\rho^2} \right] R_{m,\kappa}(\rho) = 0, \quad (14)$$

for a given value of  $m$ , the azimuthal quantum number and where  $k^2 = 2m_r E/\hbar^2$  and  $U(\rho) = 2m_r V_s(\rho)/\hbar^2$ .

For the bound states, as the energy  $E$  is negative we introduce the imaginary wavenumber  $k = i\kappa$ . As we choose a potential vanishing at large distances, the solution of the radial equation Eq. (12) can be approximated for large  $\rho$  by the solution of the free Bessel equation, which is a linear combination of the modified Bessel functions of the first and second kind. Then, the solution of the radial Schrödinger, Eq. (12), can be written as follows [22]:

$$R_{m,\kappa}(\rho) = A_m \left( I_m(\kappa\rho) \cos \eta_m + \frac{2}{\pi} K_m(\kappa\rho) \sin \eta_m \right), \quad (15)$$

where  $I_m(\kappa\rho)$  and  $K_m(\kappa\rho)$  are the modified Bessel functions of the first and second kinds respectively while the phase shift  $\eta_m$  characterises their admixture and  $A_m$  is the wavefunction amplitude.

To solve the problem for all  $\rho$ , not just  $\rho \rightarrow \infty$ , the phase shift  $\eta_m$  and the amplitude  $A_m$  are both considered not as constants but as explicit functions of  $\rho$  and  $\kappa$  in the 2D formulation of the variable phase method [29]. Following Ref. [22], we insert Eq. (15) into Eq. (14) and find that the phase shift satisfies the following first order, non-linear differential equation of the Riccati type:

$$\frac{d}{d\rho} \eta_{m,\kappa}(\rho) = -\frac{\pi}{2} \rho U(\rho) \times \left( I_m(\kappa\rho) \cos \eta_{m,\kappa}(\rho) + \frac{2}{\pi} K_m(\kappa\rho) \sin \eta_{m,\kappa}(\rho) \right)^2.$$

Eq. (16) is called the phase equation and should be solved with the boundary condition:

$$\eta_{m,\kappa}(0) = 0, \quad (16)$$

thus ensuring that the radial function does not diverge at  $\rho = 0$ .

For the bound states the diverging solution vanishes, thus implying the asymptotic condition:

$$\lim_{\rho \rightarrow \infty} \eta_{m,\kappa}(\rho) = (\nu - 1/2)\pi, \quad (17)$$

where  $\nu$  enumerates the bound states for a given  $m$ . The number of non-zero nodes of the radial wave function is given by  $\nu - 1$ .

Similarly the amplitude  $A_{m,\kappa}(\rho)$  satisfies the following equation:

$$\frac{d}{d\rho} A_{m,\kappa}(\rho) = A_{m,\kappa}(\rho) \frac{I_m(\kappa\rho) \sin \eta_{m,\kappa}(\rho) - \frac{2}{\pi} K_m(\kappa\rho) \cos \eta_{m,\kappa}(\rho)}{I_m(\kappa\rho) \cos \eta_{m,\kappa}(\rho) + \frac{2}{\pi} K_m(\kappa\rho) \sin \eta_{m,\kappa}(\rho)} \times \frac{d}{d\rho} \eta_{m,\kappa}(\rho), \quad (18)$$

which is coupled to the phase equation, Eq. (16), whose

solution may be computed first.

The final expression of the relative wave function

$\psi_{m,\kappa}(\rho, \varphi)$  is:

$$\psi_{m,\kappa}(\rho, \varphi) = A_{m,\kappa}(\rho) \times \left( I_m(\kappa\rho) \cos \eta_{m,\kappa}(\rho) + \frac{2}{\pi} K_m(\kappa\rho) \sin \eta_{m,\kappa}(\rho) \right) e^{im\varphi}. \quad (19)$$

The exciton center of mass motion is characterized by the plane wave  $\phi_{\mathbf{k}_{\text{cm}}}(\mathbf{R}) = \exp(-i\mathbf{k}_{\text{cm}} \cdot \mathbf{R})/\sqrt{\mathcal{A}}$ , where  $\mathbf{R} = (m_e \mathbf{r}_e + m_h \mathbf{r}_h)/(m_e + m_h)$  is the exciton center of mass coordinate,  $\mathbf{r}_e$  and  $\mathbf{r}_h$  the carrier coordinates,  $\mathcal{A}$  is the surface area of the 2D system and  $k_{\text{cm}} = \sqrt{2M E_{\text{cm}}}/\hbar$  the exciton center of mass momentum. The total exciton wave function is the product of this plane wave and the relative wavefunction calculated above:  $\Psi_{m,\kappa,\mathbf{k}_{\text{cm}}}(\mathbf{R}, \rho, \varphi) = \phi_{\mathbf{k}_{\text{cm}}}(\mathbf{R}) \times \psi_{m,\kappa}(\rho, \varphi)$ .

## B. Scattering states

In the present case, the energy of the unbound electron-hole system is positive, and the wavenumber  $k = \sqrt{2m_e E}/\hbar$  is a positive real number. The scattering phase shift is also given by a differential equation of the Riccati type [22]:

$$\frac{d}{d\rho} \delta_{m,k}(\rho) = -\frac{\pi}{2} \rho U(\rho) (J_m(k\rho) \cos \delta_{m,k}(\rho) - N_m(k\rho) \sin \delta_{m,k}(\rho))^2, \quad (20)$$

and the amplitude satisfies the following differential equation [22]:

$$\frac{d}{d\rho} A_{m,k}(\rho) = A_{m,k}(\rho) \frac{J_m(k\rho) \sin \delta_{m,k}(\rho) + N_m(k\rho) \cos \delta_{m,k}(\rho)}{J_m(k\rho) \cos \delta_{m,k}(\rho) - N_m(k\rho) \sin \delta_{m,k}(\rho)} \times \frac{d}{d\rho} \delta_{m,k}(\rho), \quad (21)$$

where  $J_m$  and  $N_m$  are the Bessel and Neumann functions.

The scattering wave function as function of electron-hole separation in a 2D screened Coulomb potential is:

$$\psi_{m,k}(\rho, \varphi) = A_{m,k}(\rho) e^{im\varphi} (J_m(k\rho) \cos \delta_{m,k}(\rho) - N_m(k\rho) \sin \delta_{m,k}(\rho)). \quad (22)$$

The knowledge of the scattering states  $\psi_{m,k}(\rho, \varphi)$  is required to compute the Sommerfeld factor. At the band edge, for  $m = 0$ , the 2D Coulomb enhancement yields a factor of two if there is no plasma screening [35]. At finite density the enhancement is reduced and lies between two and one (see Table 1).

## IV. THE CONTRIBUTION OF EXCITON-ELECTRON SCATTERING TO PL

### A. The scattering matrix elements

In this section we are concerned with the scattering of  $1s$  excitons with free electrons: the excitons transfer their momenta and energies to the free electrons, and reach the photon line where they recombine with the emission of

a photon. The carriers interact via the screened potentials defined in Eq. (2). Coulomb attraction between the free electron and the bound hole, Coulomb repulsion between the free electron and the bound electron as well as

---


$$V_{\text{scat}} = \frac{1}{2} \int d\mathbf{r}_1 d\mathbf{r}_2 d\mathbf{r}_h \left( \phi_{\mathbf{k}_2 + \mathbf{k}_{\text{cm}}}^\dagger(\mathbf{r}_2) \Psi_{0, \kappa, \vec{0}}^\dagger(\vec{0}, \rho_{1h}) - \phi_{\mathbf{k}_1 + \mathbf{k}_{\text{cm}}}^\dagger(\mathbf{r}_1) \Psi_{0, \kappa, \vec{0}}^\dagger(\vec{0}, \rho_{2h}) \right) \times (V_s(\rho_{1h}) + V_s(\rho_{2h}) + V_s(\rho_{12})) (\Psi_{0, \kappa, \mathbf{k}_{\text{cm}}}(\mathbf{R}_1, \rho_{1h}) \phi_{\mathbf{k}_2}(\mathbf{r}_2) - \Psi_{0, \kappa, \mathbf{k}_{\text{cm}}}(\mathbf{R}_2, \rho_{2h}) \phi_{\mathbf{k}_1}(\mathbf{r}_1)), \quad (23)$$


---

where  $\mathbf{R}_1$  and  $\mathbf{R}_2$  are the exciton centers of mass coordinates,  $\mathbf{r}_1$  and  $\mathbf{r}_2$  the electrons coordinates and  $\mathbf{r}_h$  the hole coordinate. The relative distances are defined as follows:  $\rho_{1h} = \|\mathbf{r}_h - \mathbf{r}_1\|$ ,  $\rho_{2h} = \|\mathbf{r}_h - \mathbf{r}_2\|$  and  $\rho_{12} = \|\mathbf{r}_1 - \mathbf{r}_2\|$ . Note that the attractive electron-hole interaction potentials  $V_s(\rho_{1h})$  and  $V_s(\rho_{2h})$  are negative and the repulsive electron-electron interaction potential  $V_s(\rho_{12})$  is positive. Since we consider  $1s$  exciton states only, the value of the projection of the angular momentum,  $m$ , is zero and we remove the explicit  $\varphi$  dependence from the expression of  $\Psi_{0, \kappa, \mathbf{k}_{\text{cm}}}$ . The initial state of the free electron is the plane wave  $\phi_{\mathbf{k}}$  characterized by the wavevector  $\mathbf{k}$  ( $= \mathbf{k}_1$  or  $\mathbf{k}_2$ ), and its final state the plane wave  $\phi_{\mathbf{k} + \mathbf{k}_{\text{cm}}}$  characterized by  $\mathbf{k} + \mathbf{k}_{\text{cm}}$ , where  $\mathbf{k}_{\text{cm}}$  is the exciton center of mass momentum that has been transferred during the scattering process. Equation (23) is similar to the expression in Ref. [28].

As shown in Appendix A the matrix element  $V_{\text{scat}}$  can be written as a sum of a direct term  $V_{\text{scat}}^{\text{dir}}$  and an exchange term  $V_{\text{scat}}^{\text{exch}}$ , and evaluation of the integrals in Eq. 23 reduces to

$$V_{\text{scat}}^{\text{dir}}(k_{\text{cm}}, \kappa) = \frac{e^2}{16\pi^3 \epsilon_0 \epsilon_r} \frac{\widetilde{R}_{0, \kappa}^2 \left( \frac{m_h}{M} k_{\text{cm}} \right) - \widetilde{R}_{0, \kappa}^2 \left( \frac{m_e}{M} k_{\text{cm}} \right)}{k_{\text{cm}} + q_s}, \quad (24)$$


---

exchange between the two electrons are included in the calculation of the scattering matrix element  $V_{\text{scat}}$  whose general expression can be written as follows:

---

where the quantity  $\widetilde{R}_0^2$  denotes the Fourier transform of the square of the  $m = 0$  radial wavefunction in Eq. (13). Since we neglect the exchange contribution  $V_{\text{scat}}$  is independent of the scattering free electron momentum  $\mathbf{k}$  and only depends on the energy of the bound state characterized by the wavenumber  $\kappa$ , effective masses of the carriers  $m_e$  and  $m_h$ , and the initial momentum  $k_{\text{cm}}$ .

## B. Exciton-electron scattering contribution to SER

The next step of the calculations consists of evaluating the contribution of the scattering of excitons and electrons to the spontaneous emission,  $R_{\text{sp}}^{\text{corr}}$ . The contribution of the correlated particles in the plasma,  $R_{\text{sp}}^{\text{corr}}$ , is calculated combining Eqs. (10-13). In the Boltzmann limit the matrix elements are dominated by the direct terms which yields:

---


$$R_{\text{sp}}^{\text{corr}}(\hbar\Omega) = \frac{2\pi}{\hbar} F(\Omega) \times \sum_{\mathbf{k}_{\text{cm}}} \frac{2\pi\beta\hbar^2}{M} (1 - \alpha) N \exp\left(-\beta \frac{\hbar^2 k_{\text{cm}}^2}{2M}\right) |V_{\text{scat}}(k_{\text{cm}})|^2 \times \sum_{\mathbf{k}_2} \frac{2\pi\beta\hbar^2}{m_e} \alpha N \exp\left(-\beta \frac{\hbar^2 k_2^2}{2m_e}\right) \delta\left(E_g - E_b^X + \frac{\hbar^2 k_{\text{cm}}^2}{2M} - \hbar\Omega - \frac{\hbar^2}{2m_e}(k_{\text{cm}}^2 + 2\mathbf{k}_{\text{cm}} \cdot \mathbf{k}_2)\right), \quad (25)$$


---

As shown in Appendix B this can be reduced to:

$$R_{\text{sp}}^{\text{corr}}(\hbar\Omega) = \frac{F(\Omega)\alpha(1-\alpha)N^2\sqrt{2\pi m_e\beta^3}}{M} \int_0^\infty e^{-\beta \left[ \frac{\hbar^2 k_{\text{cm}}^2}{2M} + \frac{m_e}{2\hbar^2 k_{\text{cm}}^2} \left( E_g - E_b^X - \hbar\Omega - \frac{m_h}{m_e} \frac{\hbar^2 k_{\text{cm}}^2}{2M} \right)^2 \right]} |V_{\text{scat}}(k_{\text{cm}})|^2 dk_{\text{cm}}. \quad (26)$$

$R_{\text{sp}}^{\text{corr}}(\hbar\Omega)$  depends explicitly on the degree of ionization,  $\alpha$ , via the product  $\alpha(1-\alpha)$ . This product is maximum for  $\alpha = 1/2$ , which means that for given thermodynamic conditions on temperature and density,  $R_{\text{sp}}^{\text{corr}}(\hbar\Omega)$ , as defined above, is greater when the plasma is composed of a mixture of excitons and free carriers in equal proportions. As mentioned in section II.B, the nature of the electron-hole plasma in ZnSe QWs is closer to a plasma with  $\alpha = 1/2$  than it is in GaAs QWs, and one should expect a more important contribution of exciton-electron scattering to PL in ZnSe QWs. Note that very high proportion of excitons do not guarantee a great contribution to  $R_{\text{sp}}^{\text{corr}}(\hbar\Omega)$  either, as it would simply mean that there would not be enough free carriers to scatter with. The key point here is to have  $\alpha$  close to 1/2.

## V. NUMERICAL RESULTS

The materials parameters for GaAs-based quantum-wells are:  $m_e = 0.067m_0$ ,  $m_h = 0.46m_0$ , where  $m_0$  is the free electron mass,  $\epsilon_r = 12$ ,  $E_g = 1.45$  eV,  $x_{vc} = 5.0$  Å and  $n_{\text{op}} = 3.6$ . For ZnSe we use:  $m_e = 0.15m_0$ ,  $m_h = 0.60m_0$ ,  $\epsilon_r = 8.8$ ,  $E_g = 2.7$  eV and  $x_{vc} = 3.0$  Å and  $n_{\text{op}} = 2.5$ . As in Ref. [14] we take  $\beta_1 \approx 10^{-3}$ . The ionization degree is evaluated at  $T = 300$  K for various plasma densities given in Table 1.

### A. The scattering matrix element

In Fig. 2 the behavior of the scattering matrix element versus  $k_{\text{cm}}$  is shown for two values of the plasma screening:  $q_s a_B = 0.1$  and  $q_s a_B = 2.5$ , for both materials.

In all cases the qualitative behavior of  $V_{\text{scat}}$  is the same:  $V_{\text{scat}} = 0$  for  $k_{\text{cm}} = 0$  since the exciton cannot scatter from  $k_{\text{cm}} = 0$  to  $k_{\text{cm}} = 0$ ; then for low values of the wavenumber,  $V_{\text{scat}}$  which is negative for all values of  $k_{\text{cm}}$ , decreases and reaches a minimum for values of  $k_{\text{cm}}$  that are close (around  $3 a_B^{-1}$ ); this means that the location of the minimum mostly depends on the ratio of the electron and hole effective masses, and less on the screening parameter in the low density regime; for values greater than  $3 a_B^{-1}$ ,  $V_{\text{scat}}$  is an increasing function of  $k_{\text{cm}}$  whose amplitude diminishes: the transfer of increasing large exciton center of mass momentum to its scattering partner is less likely. The matrix element  $V_{\text{scat}}$  is, as expected, greater for low screening, but not in a dramatic way: in the low density regime the screening parameter remains small enough not to have a significant impact

on the amplitude of  $V_{\text{scat}}$ . The magnitude of  $V_{\text{scat}}$  is also higher in ZnSe than it is in GaAs, reflecting the greater strength of Coulomb interaction in ZnSe. Note that if the electron and hole effective masses were equal, the electron-electron and electron-hole contributions to  $V_{\text{scat}}$  would cancel exactly and the scattering amplitude would be zero for all  $k_{\text{cm}}$ .

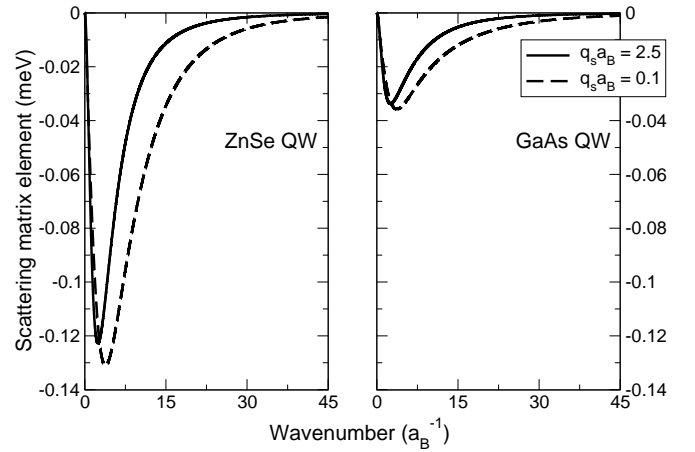


FIG. 2: Scattering matrix element as function of wavenumber, describing the 1s exciton-electron scattering with a screened Coulomb potential in ZnSe and GaAs quantum wells, in a low density regime at  $T = 300$  K.

### B. The electron-hole contribution to the spontaneous emission rate

The electron-hole spontaneous emission rate,  $R_{\text{sp}}^{\text{eh}}(\hbar\Omega)$ , depicted in Fig. (3), decreases with decreasing density at a given temperature and depends on the material parameters such as the bandgap and the dielectric constant, through the radiative lifetime  $\tau_{\text{rad}}$ . The computed spectra take Coulomb enhancement at the band edge and above into account. For ZnSe,  $\tau_{\text{rad}}$  is smaller than for GaAs. Hence, the PL spectra shows that for the same scaled density, and at a given temperature, the PL signals are greater for ZnSe than they are for GaAs. The electron-hole contribution shows a thermal tail on the high energy side of the emission line.

TABLE I: Values of plasma screening parameter  $q_s$  scaled to the excitonic Bohr radius, and the corresponding densities  $N$  in  $10^{11}\text{cm}^{-2}$  and degrees of ionization  $\alpha$ , for ZnSe and GaAs QWs at  $T = 300$  K. The exciton binding energies,  $E_b^X$ , are given in excitonic Rydbergs. Values of  $|\psi_E(\rho = 0)|^2$  are also given for angular momentum  $m = 0$  and energy  $E = 0$ .

GaAs			ZnSe			$E_b^X$	$ \psi_E(\rho = 0) ^2$
$q_s a_B$	$N$	$\alpha(N)$	$N$	$\alpha(N)$			
0.10	0.14	0.93	0.66	0.41	3.30	1.81	
0.32	0.48	0.86	2.51	0.34	2.51	1.60	
1.0	1.62	0.78	6.78	0.39	1.35	1.30	
1.25	2.06	0.77	8.0	0.41	1.05	1.21	
2.5	4.27	0.74	13.31	0.50	0.38	1.13	

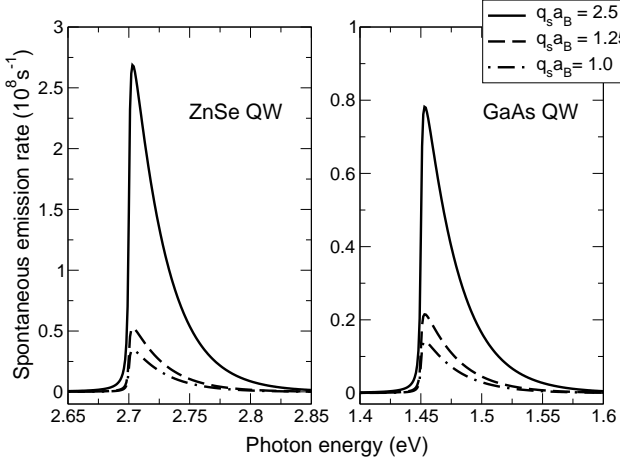


FIG. 3: EHP contribution to the spontaneous emission rate evaluated for GaAs and ZnSe in the Boltzmann regime at  $T = 300$  K. The corresponding values of the densities for the screening parameters are given in Table I. For a given plasma density the spontaneous emission rate in ZnSe is much greater than it is for GaAs. Note the differing vertical scales.

### C. The exciton contribution to the spontaneous emission rate

The numerical evaluation of Eq. (26) gives the exciton contribution to the spontaneous emission rate, due to exciton-electron scattering as shown in Fig. 4. For a given material the behavior of  $R_{\text{sp}}^{\text{corr}}(\hbar\Omega)$  reflects its complex density dependence via  $\alpha(N)(1 - \alpha(N))N^2$ . Note that since the scattering matrix element does not depend dramatically on  $N$  it has a rather small influence on the spontaneous emission rate:  $R_{\text{sp}}^{\text{corr}}(\hbar\Omega)$  is proportional to the square of  $V_{\text{scat}}$  and while  $V_{\text{scat}}$  decreases with increasing plasma density,  $R_{\text{sp}}^{\text{corr}}(\hbar\Omega)$  is increasing significantly. Comparing results obtained for ZnSe and GaAs, it appears clearly that the exciton contribution to the spontaneous emission rate at room temperature is much more important in ZnSe than it is in GaAs. This is due to the fact that with a smaller dielectric constant the Coulomb interaction is greater in ZnSe QWs where the exciton population remains important at moderate carrier densities whereas the fraction of excitons in GaAs QWs is too modest to yield a significant excitonic contribution

to PL. Note that the correlated contribution has a thermal tail on the low energy side of the spectrum mirroring the free electron distribution function.

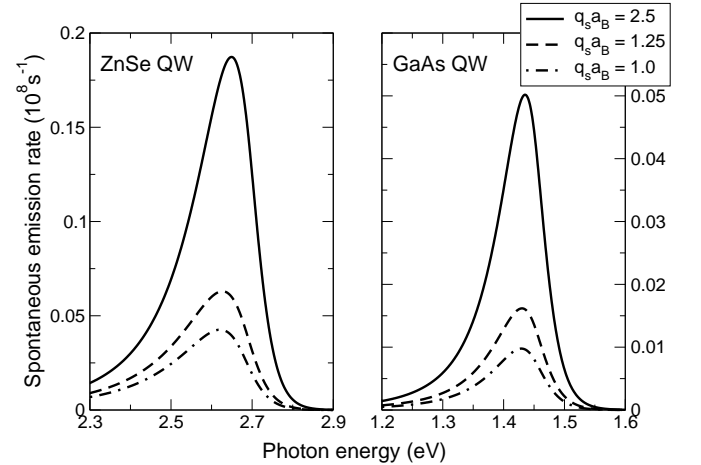


FIG. 4: Contribution of the 1s exciton-electron scattering to the spontaneous emission rate evaluated for GaAs and ZnSe in the Boltzmann regime for  $T = 300$  K. The corresponding values of the densities for the screening parameters are given in Table I. Note that for a given plasma density the contribution of the correlations to the spontaneous emission rate in ZnSe QW is much more important than it is in GaAs QW. Note the differing vertical scales.

### D. Comparison of EHP and XES contributions

In Fig. 5, the spontaneous emission rates are obtained by adding contributions from  $R_{\text{sp}}^{\text{eh}}$  and  $R_{\text{sp}}^{\text{corr}}$ . They are shown normalized in order to compare the relative importance of the contribution of the 1s exciton-electron scattering contribution for various densities. A significant peak appears below the band edge only for ZnSe. As mentioned earlier, this is due to the more important exciton population at room temperature because of the large binding energy and greater scattering matrix elements. Hence, GaAs and ZnSe exhibit different qualitative behaviors at room temperature: excitonic processes have to be taken into account for ZnSe.

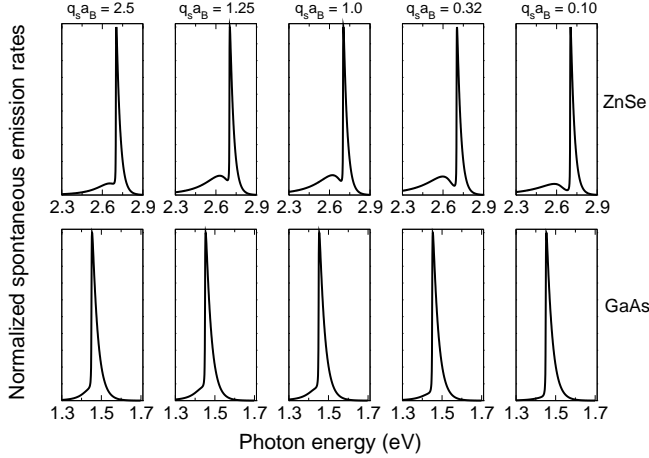


FIG. 5: Comparison of XES and EHP contributions to the spontaneous emission rate evaluated for GaAs and ZnSe in the Boltzmann regime for  $T = 300$  K. The corresponding values of the densities for the screening parameters are given in Table I.

The lower the density is, the lower the plasma screening is and the stronger the Coulomb interaction is; moreover, the free-carrier spontaneous emission rate rapidly decreases with a decreasing density. This explains why the exciton peak becomes relatively more important at low density. However, the fact that the scaled exciton peak is more important for  $q_s a_B = 0.32$  than it is for  $q_s a_B = 0.10$ , reflects the non-monotonic behaviour of the ionization degree as a function of density for ZnSe: the presence of a minimum at low density in Fig. 1 implies that the excitonic population is at its maximum as is its relative contribution to PL via scattering with electrons.

Also note that the use of a simple static screening, such as is employed here to facilitate the scattering phase shift calculations, leads to a gross overestimate of the renormalisation and a resultant red-shift of the exciton line [36]. This is not seen in experiment and is a consequence of the static approximation. To circumvent this difficulty we exploited the Ward identities which indicate that the

exciton line remains fixed and so we combined the excitonic and EHP components accordingly, i.e. the origin of the EHP component lies precisely one exciton binding energy above the exciton line. In this way energy renormalisation is included in the calculation in a physically correct fashion, albeit somewhat ad-hoc way.

## VI. CONCLUSION

We have computed and compared the contributions of electron-hole plasma and exciton-electron scattering to the spontaneous emission rate for GaAs-based and ZnSe-based QWs at room temperature, in a low density regime. The SER exhibit a significant peak below the band edge for ZnSe QWs. Therefore, inclusion of electron-hole Coulomb correlations such as excitons appears to be crucial for the study of wide-gap materials whereas simpler models described in Refs. [3, 6] are sufficient for mid- and certainly narrow gap materials at room temperature. Object of further work would be to include carrier-phonon and exciton-phonon scattering in the model presented above as one might expect a non-negligible influence of lattice vibrations on the emission mechanisms at room temperature.

## Acknowledgements

We acknowledge support from the UK EPSRC. H. O. also acknowledges partial support from Science Foundation Ireland during his stay at the Tyndall National Institute (ex National Microelectronics Research Center) Cork, Ireland. M.E.P. acknowledges the hospitality of the ICCMP's staff and the financial support received from MCT and FINEP (Brazil).

## APPENDIX A: CALCULATION OF THE SCATTERING MATRIX ELEMENTS

We start from Eq. (23):

$$V_{\text{scat}} = \frac{1}{2} \int d\mathbf{r}_1 d\mathbf{r}_2 d\mathbf{r}_h \left( \phi_{\mathbf{k}_2 + \mathbf{k}_{\text{cm}}}^\dagger(\mathbf{r}_2) \Psi_{0, \kappa, \vec{0}}^\dagger(\vec{0}, \rho_{1h}) - \phi_{\mathbf{k}_1 + \mathbf{k}_{\text{cm}}}^\dagger(\mathbf{r}_1) \Psi_{0, \kappa, \vec{0}}^\dagger(\vec{0}, \rho_{2h}) \right) \times (V_s(\rho_{1h}) + V_s(\rho_{2h}) + V_s(\rho_{12})) (\Psi_{0, \kappa, \mathbf{k}_{\text{cm}}}(\mathbf{R}_1, \rho_{1h}) \phi_{\mathbf{k}_2}(\mathbf{r}_2) - \Psi_{0, \kappa, \mathbf{k}_{\text{cm}}}(\mathbf{R}_2, \rho_{2h}) \phi_{\mathbf{k}_1}(\mathbf{r}_1)). \quad (\text{A1})$$

The first step consists of identifying the relevant physical terms: the direct and exchange terms,  $V_{\text{scat}}^{\text{dir}}$  and  $V_{\text{scat}}^{\text{exch}}$

respectively. Calculations yield the following expressions:

$$V_{\text{scat}}^{\text{dir}} = \int \phi_{\mathbf{k}_2 + \mathbf{k}_{\text{cm}}}^{\dagger}(\mathbf{r}_2) \Psi_{0, \kappa, \vec{0}}^{\dagger}(\vec{0}, \rho_{1h}) (V_s(\rho_{2h}) + V_s(\rho_{12})) \Psi_{0, \kappa, \mathbf{k}_{\text{cm}}}(\mathbf{R}_1, \rho_{1h}) \phi_{\mathbf{k}_2}(\mathbf{r}_2) \, d\mathbf{r}_1 d\mathbf{r}_2 d\mathbf{r}_h \quad (\text{A2})$$

and

$$V_{\text{scat}}^{\text{exch}} = - \int \phi_{\mathbf{k}_2 + \mathbf{k}_{\text{cm}}}^{\dagger}(\mathbf{r}_2) \Psi_{0, \kappa, \vec{0}}^{\dagger}(\vec{0}, \rho_{1h}) (V_s(\rho_{1h}) + V_s(\rho_{2h}) + V_s(\rho_{12})) \Psi_{0, \kappa, \mathbf{k}_{\text{cm}}}(\mathbf{R}_2, \rho_{2h}) \phi_{\mathbf{k}_1}(\mathbf{r}_1) \, d\mathbf{r}_1 d\mathbf{r}_2 d\mathbf{r}_h. \quad (\text{A3})$$

An additional term  $V_{\text{scat}}^{\text{add}}$  appears:

$$V_{\text{scat}}^{\text{add}} = \int \phi_{\mathbf{k}_2 + \mathbf{k}_{\text{cm}}}^{\dagger}(\mathbf{r}_2) \Psi_{0, \kappa, \vec{0}}^{\dagger}(\vec{0}, \rho_{1h}) V_s(\rho_{1h}) \Psi_{0, \kappa, \mathbf{k}_{\text{cm}}}(\mathbf{R}_1, \rho_{1h}) \phi_{\mathbf{k}_2}(\mathbf{r}_2) \, d\mathbf{r}_1 d\mathbf{r}_2 d\mathbf{r}_h, \quad (\text{A4})$$

and before proceeding with the calculations of  $V_{\text{scat}}^{\text{dir}}$  and  $V_{\text{scat}}^{\text{exch}}$ , we show that  $V_{\text{scat}}^{\text{add}}$  which has no physical meaning is in fact equal to zero. Recalling the explicit expression

of the exciton wavefunction,  $\Psi_{m, \kappa, \mathbf{k}_{\text{cm}}}$ , in Section III, the additional term may be rewritten as:

$$V_{\text{scat}}^{\text{add}} = \frac{1}{\mathcal{A}^2} \int e^{i(\mathbf{k}_{\text{cm}} + \mathbf{k}_2) \cdot \mathbf{r}_2} R_{0, \kappa}^2(\rho_{1h}) V_s(\rho_{1h}) e^{i\mathbf{k}_{\text{cm}} \cdot \mathbf{R}_1} e^{-i\mathbf{k}_2 \cdot \mathbf{r}_2} \, d\mathbf{r}_1 d\mathbf{r}_2 d\mathbf{r}_h. \quad (\text{A5})$$

We define the Fourier transforms of the square of the relative motion part of the excitonic wavefunction, Eq. (13):

$$\begin{aligned} R_{0, \kappa}^2(\rho_{1h}) &= \sum_{\mathbf{q}_1} \widetilde{R}_{0, \kappa}^2(\mathbf{q}_1) e^{i\mathbf{q}_1 \cdot (\mathbf{r}_h - \mathbf{r}_1)} \\ &= \frac{\mathcal{A}}{4\pi^2} \int \widetilde{R}_{0, \kappa}^2(\mathbf{q}_1) e^{i\mathbf{q}_1 \cdot (\mathbf{r}_h - \mathbf{r}_1)} d\mathbf{q}_1, \end{aligned} \quad (\text{A6})$$

and of the scattering potential  $V_s(\rho_-)$ :

$$\begin{aligned} V_s(\rho_{1h}) &= \sum_{\mathbf{q}} \widetilde{V}_s(\mathbf{q}) e^{i\mathbf{q} \cdot (\mathbf{r}_h - \mathbf{r}_1)} \\ &= \frac{\mathcal{A}}{4\pi^2} \int \widetilde{V}_s(\mathbf{q}) e^{i\mathbf{q} \cdot (\mathbf{r}_h - \mathbf{r}_1)} d\mathbf{q}, \end{aligned} \quad (\text{A7})$$

that we include into Eq. (A5) to find:

$$V_{\text{scat}}^{\text{add}} = \frac{1}{16\pi^4} \iint e^{i\mathbf{k}_{\text{cm}} \cdot \mathbf{r}_2} e^{-i(m_e \mathbf{k}_{\text{cm}}/M + \mathbf{q}_1 + \mathbf{q}) \cdot \mathbf{r}_1} e^{-i(m_h \mathbf{k}_{\text{cm}}/M - \mathbf{q}_1 - \mathbf{q}) \cdot \mathbf{r}_h} \widetilde{R}_{0, \kappa}^2(\mathbf{q}_1) \widetilde{V}_s(\mathbf{q}) \, d\mathbf{r}_1 d\mathbf{r}_2 d\mathbf{r}_h d\mathbf{q}_1 d\mathbf{q}. \quad (\text{A8})$$

Considering the identity  $\int e^{i\mathbf{q} \cdot \mathbf{r}} d\mathbf{r} = \delta(\mathbf{q})$ , where  $\delta$  denotes the Dirac function, the above integral reads:

$$V_{\text{scat}}^{\text{add}} = \frac{1}{16\pi^4} \iint \delta\left(\frac{m_e}{m_e + m_h} \mathbf{k}_{\text{cm}} + \mathbf{q}_1 + \mathbf{q}\right) \delta\left(-\frac{m_h}{m_e + m_h} \mathbf{k}_{\text{cm}} + \mathbf{q}_1 + \mathbf{q}\right) e^{i\mathbf{k}_{\text{cm}} \cdot \mathbf{r}_2} \widetilde{R}_{0,\kappa}^2(\mathbf{q}) \widetilde{V}_s(\mathbf{q}) \, d\mathbf{r}_2 d\mathbf{q}_1 d\mathbf{q}, \quad (\text{A9})$$

and, since  $\int \delta(a-x)\delta(b-x)f(x) \, dx = 0$  when  $a \neq b$ , we finally find that  $V_{\text{scat}}^{\text{add}} = 0$ .

### 1. The exchange term

We turn now to the exchange term  $V_{\text{scat}}^{\text{exch}}$  that we artificially decompose into three terms:  $V_{\text{scat}}^{\text{exch}} = V_{\text{scat}}^{\text{exch},1} +$

$$V_{\text{scat}}^{\text{exch},1} = - \int \phi_{\mathbf{k}_2 + \mathbf{k}_{\text{cm}}}^\dagger(\mathbf{r}_2) \Psi_{0,\kappa,\vec{0}}^\dagger(\vec{0}, \rho_{1h}) V_s(\rho_{1h}) \Psi_{0,\kappa,\mathbf{k}_{\text{cm}}}(\mathbf{R}_2, \rho_{2h}) \phi_{\mathbf{k}_1}(\mathbf{r}_1) \, d\mathbf{r}_1 d\mathbf{r}_2 d\mathbf{r}_h, \quad (\text{A10})$$

$$V_{\text{scat}}^{\text{exch},2} = - \int \phi_{\mathbf{k}_2 + \mathbf{k}_{\text{cm}}}^\dagger(\mathbf{r}_2) \Psi_{0,\kappa,\vec{0}}^\dagger(\vec{0}, \rho_{1h}) V_s(\rho_{2h}) \Psi_{0,\kappa,\mathbf{k}_{\text{cm}}}(\mathbf{R}_2, \rho_{2h}) \phi_{\mathbf{k}_1}(\mathbf{r}_1) \, d\mathbf{r}_1 d\mathbf{r}_2 d\mathbf{r}_h, \quad (\text{A11})$$

and

$$V_{\text{scat}}^{\text{exch},3} = - \int \phi_{\mathbf{k}_2 + \mathbf{k}_{\text{cm}}}^\dagger(\mathbf{r}_1) \Psi_{0,\kappa,\vec{0}}^\dagger(\vec{0}, \rho_{1h}) V_s(\rho_{12}) \Psi_{0,\kappa,\mathbf{k}_{\text{cm}}}(\mathbf{R}_2, \rho_{2h}) \phi_{\mathbf{k}_1}(\mathbf{r}_1) \, d\mathbf{r}_1 d\mathbf{r}_2 d\mathbf{r}_h. \quad (\text{A12})$$

In the same fashion as above we define the Fourier transforms:

$$\begin{aligned} R_{0,\kappa}(\rho_{1h}) &= \sum_{\mathbf{q}_1} \widetilde{R}_{0,\kappa}(\mathbf{q}_1) e^{i\mathbf{q}_1 \cdot (\mathbf{r}_h - \mathbf{r}_1)} \\ &= \frac{\mathcal{A}}{4\pi^2} \int \widetilde{R}_{0,\kappa}(\mathbf{q}_1) e^{i\mathbf{q}_1 \cdot (\mathbf{r}_h - \mathbf{r}_1)} d\mathbf{q}_1, \end{aligned} \quad (\text{A13})$$

$$\begin{aligned} R_{0,\kappa}(\rho_{2h}) &= \sum_{\mathbf{q}_2} \widetilde{R}_{0,\kappa}(\mathbf{q}_2) e^{i\mathbf{q}_2 \cdot (\mathbf{r}_h - \mathbf{r}_2)} \\ &= \frac{\mathcal{A}}{4\pi^2} \int \widetilde{R}_{0,\kappa}(\mathbf{q}_2) e^{i\mathbf{q}_2 \cdot (\mathbf{r}_h - \mathbf{r}_2)} d\mathbf{q}_2, \end{aligned} \quad (\text{A14})$$

$$\begin{aligned} V_s(\rho_{2h}) &= \sum_{\mathbf{q}} \widetilde{V}_s^-(\mathbf{q}) e^{i\mathbf{q} \cdot (\mathbf{r}_h - \mathbf{r}_2)} \\ &= \frac{\mathcal{A}}{4\pi^2} \int \widetilde{V}_s^-(\mathbf{q}) e^{i\mathbf{q} \cdot (\mathbf{r}_h - \mathbf{r}_2)} d\mathbf{q}, \end{aligned} \quad (\text{A15})$$

$$\begin{aligned} V_s(\rho_{12}) &= \sum_{\mathbf{q}} \widetilde{V}_s^+(\mathbf{q}) e^{i\mathbf{q} \cdot (\mathbf{r}_2 - \mathbf{r}_1)} \\ &= \frac{\mathcal{A}}{4\pi^2} \int \widetilde{V}_s^+(\mathbf{q}) e^{i\mathbf{q} \cdot (\mathbf{r}_2 - \mathbf{r}_1)} d\mathbf{q}, \end{aligned} \quad (\text{A16})$$

where the + and - signs denote the repulsive and attractive potentials. Inserting the relevant Fourier transforms

of Eqs. (A6), (A7), (A13-A16) into Eqs. (A10), (A11) and (A12) and performing the same type of calculations

as for  $V_{\text{scat}}^{\text{add}}$ , we find:

$$V_{\text{scat}}^{\text{exch},1} = -\frac{1}{\mathcal{A}} \int \tilde{R}_{0,\kappa}(-\mathbf{k}_2 - \mathbf{q}) \tilde{R}_{0,\kappa}(\mathbf{k}_2 + \frac{m_h \mathbf{k}_{\text{cm}}}{m_e + m_h} + \mathbf{q}) \tilde{V}_s(\mathbf{q}) d\mathbf{q}, \quad (\text{A17})$$

$$V_{\text{scat}}^{\text{exch},2} = -\frac{1}{\mathcal{A}} \tilde{R}_{0,\kappa}(\mathbf{k}_2 + \frac{m_h \mathbf{k}_{\text{cm}}}{m_e + m_h}) \int \tilde{R}_{0,\kappa}(-\mathbf{k}_2 - \mathbf{q}) \tilde{V}_s^-(\mathbf{q}) d\mathbf{q}, \quad (\text{A18})$$

and

$$V_{\text{scat}}^{\text{exch},3} = -\frac{1}{\mathcal{A}} \tilde{R}_{0,\kappa}(\mathbf{k}_2) \int \tilde{R}_{0,\kappa}(\mathbf{k}_2 + \frac{m_h \mathbf{k}_{\text{cm}}}{m_e + m_h} - \mathbf{q}) \tilde{V}_s^+(\mathbf{q}) d\mathbf{q}. \quad (\text{A19})$$

The exchange term,  $V_{\text{scat}}^{\text{exch}}$ , depends on the properties of each scattering partner: exciton binding energy, kinetic energies, effective masses of the electrons, hole and exciton.

$V_{\text{scat}}^+ + V_{\text{scat}}^-$  and we need only to explicit calculations for  $V_{\text{scat}}^+$  as  $V_{\text{scat}}^+$  has a similar structure.  $V_{\text{scat}}^-$  is the first of the two terms in Eq. (A2):

## 2. Direct term

Finally, we show the main steps of the calculation of the direct term starting from Eq. (A2). We write  $V_{\text{scat}}^{\text{dir}} =$

$$V_{\text{scat}}^- = \int \phi_{\mathbf{k}_2 + \mathbf{k}_{\text{cm}}}^\dagger(\mathbf{r}_2) \Psi_{0,\kappa,\sigma}^\dagger(\vec{0}, \rho_{1h}) V_s(\rho_{2h}) \Psi_{0,\kappa,\mathbf{k}_{\text{cm}}}(\mathbf{R}_1, \rho_{1h}) \phi_{\mathbf{k}_2}(\mathbf{r}_2) d\mathbf{r}_1 d\mathbf{r}_2 d\mathbf{r}_h \quad (\text{A20})$$

Using the explicit expressions of the electron plane wave and exciton wavefunction of Section III as well as the def-

initions of the Fourier tranforms of Eqs. (A6) and (A15), we find:

$$V_{\text{scat}}^- = \frac{1}{16\pi^4} \int e^{i(\mathbf{k}_{\text{cm}} + \mathbf{q}) \cdot \mathbf{r}_{e2}} e^{i(\mathbf{q}_1 - m_e \mathbf{k}_{\text{cm}}/M) \cdot \mathbf{r}_1} e^{-i(\mathbf{q} + \mathbf{q}_1 + m_h \mathbf{k}_{\text{cm}}/M) \cdot \mathbf{r}_h} \tilde{R}_{0,\kappa}^2(\mathbf{q}) \tilde{V}_s^-(\mathbf{q}) d\mathbf{r}_1 d\mathbf{r}_2 d\mathbf{r}_h d\mathbf{q} d\mathbf{q}_1. \quad (\text{A21})$$

This 10-dimensional integral can be simplified using again the definition the  $\delta$ -function given above:

$$V_{\text{scat}}^- = \frac{\mathcal{A}}{16\pi^4} \tilde{R}_{0,\kappa}^2(\frac{m_e \mathbf{k}_{\text{cm}}}{M}) \tilde{V}_s^-(\mathbf{k}_{\text{cm}}). \quad (\text{A22})$$

Doing the same calculations with  $V_{\text{scat}}^+$ , Eq. (A2) can be reduced to the following expression in the Fourier space:

$$V_{\text{scat}}^{\text{dir}}(\mathbf{k}_{\text{cm}}, \kappa) = \frac{\mathcal{A}}{16\pi^4} \left( \tilde{R}_{0,\kappa}^2(\frac{m_e \mathbf{k}_{\text{cm}}}{M}) \tilde{V}_s^-(\mathbf{k}_{\text{cm}}) + \tilde{R}_{0,\kappa}^2(-\frac{m_h \mathbf{k}_{\text{cm}}}{M}) \tilde{V}_s^+(\mathbf{k}_{\text{cm}}) \right). \quad (\text{A23})$$

Combining Eq. (A23) with the Fourier transform of Eq. (2) and performing the integration of  $V_{\text{scat}}^{\text{dir}}(\mathbf{k}_{\text{cm}}, \kappa)$

over  $[0; 2\pi]$  yield the final expression of the direct term:

$$V_{\text{scat}}^{\text{dir}}(k_{\text{cm}}, \kappa) = \frac{e^2}{16\pi^3 \epsilon_0 \epsilon_r} \frac{\tilde{R}_{0,\kappa}^2(\frac{m_h k_{\text{cm}}}{M}) - \tilde{R}_{0,\kappa}^2(\frac{m_e k_{\text{cm}}}{M})}{k_{\text{cm}} + q_s}. \quad (\text{A24})$$

Note that unlike the exchange term, the direct term only depends on the exciton properties: kinetic energy, binding energy and effective masses.

## APPENDIX B: CALCULATION OF $R_{\text{sp}}^{\text{corr}}$

To calculate the contribution of the correlated particles in the plasma,  $R_{\text{sp}}^{\text{corr}}$ , we start from Eq. (25):

---


$$R_{\text{sp}}^{\text{corr}}(\hbar\Omega) = \frac{2\pi}{\hbar} F(\Omega) \times \sum_{\mathbf{k}_{\text{cm}}} \frac{2\pi\beta\hbar^2}{M} (1-\alpha)N \exp\left(-\beta \frac{\hbar^2 k_{\text{cm}}^2}{2M}\right) |V_{\text{scat}}(k_{\text{cm}})|^2 \\ \times \sum_{\mathbf{k}_2} \frac{2\pi\beta\hbar^2}{m_e} \alpha N \exp\left(-\beta \frac{\hbar^2 k_2^2}{2m_e}\right) \delta\left(E_g - E_b^X + \frac{\hbar^2 k_{\text{cm}}^2}{2M} - \hbar\Omega - \frac{\hbar^2}{2m_e}(k_{\text{cm}}^2 + 2\mathbf{k}_{\text{cm}} \cdot \mathbf{k}_2)\right). \quad (\text{B1})$$


---

The first step of the calculation of Eq. (B1) is the evaluation of the discrete sum over all the vectors  $\mathbf{k}_2$ . To do

so, one can approximate the sum  $S$ :

---


$$S = \sum_{\mathbf{k}_2} \exp\left(-\beta \frac{\hbar^2 k_2^2}{2m_e}\right) \delta\left(E_g - E_b^X + \frac{\hbar^2 k_{\text{cm}}^2}{2M} - \hbar\Omega - \frac{\hbar^2}{2m_e}(k_{\text{cm}}^2 + 2\mathbf{k}_{\text{cm}} \cdot \mathbf{k}_2)\right), \quad (\text{B2})$$


---

by a 2D integral:

---


$$S = \frac{\mathcal{A}}{4\pi^2} \int_{k_2^{\min}}^{k_2^{\max}} \int_0^{2\pi} k_2 \exp\left(-\beta \frac{\hbar^2 k_2^2}{2m_e}\right) \times \delta\left(E_g - E_b^X + \frac{\hbar^2 k_{\text{cm}}^2}{2M} - \hbar\Omega - \frac{\hbar^2}{2m_e}(k_{\text{cm}}^2 + 2\mathbf{k}_{\text{cm}} \cdot \mathbf{k}_2)\right) dk_2 d\theta. \quad (\text{B3})$$


---

The integral over  $\theta$  can be calculated:

if  $|X| < |Y|$ . We apply the above result to the integral over  $\theta$  in Eq. (B3) and find:

---


$$\int_0^{2\pi} \delta(X - Y \cos\theta) d\theta = \frac{2}{|Y \sin[\cos^{-1} X/Y]|} \quad (\text{B4})$$


---

---


$$\int_0^{2\pi} \delta\left(E_g - E_b^X + \frac{\hbar^2 k_{\text{cm}}^2}{2M} - \hbar\Omega - \frac{\hbar^2}{2m_e}(k_{\text{cm}}^2 + 2\mathbf{k}_{\text{cm}} \cdot \mathbf{k}_2)\right) d\theta = \frac{2}{\left|\frac{\hbar^2}{m_e} k_{\text{cm}} k_2 \sin\left[\cos^{-1}\left(\frac{E_g - \hbar\Omega - \hbar^2 k_{\text{cm}}^2/2m_e}{\hbar^2 k_{\text{cm}} k_2/m_e}\right)\right]\right|}, \quad (\text{B5})$$


---

where  $X = E_b^X - \hbar\Omega - \hbar^2 k_{\text{cm}}^2/2m_e$ ,  $Y = \hbar^2 k_{\text{cm}} k_2/m_e$ , and with the above condition on  $X$  and  $Y$ , the

limits of the integral Eq. (B3) are:  $k_2^{\min} =$

$(E_X - \hbar\Omega - \hbar^2 k_{\text{cm}}^2/2m_e) m_e/\hbar^2 k_{\text{cm}}$  and  $k_2^{\max} \rightarrow \infty$ .

Considering the identity  $|\sin[\cos^{-1} \Theta]| = \sqrt{1 - \cos^2[\cos^{-1} \Theta]} = \sqrt{1 - \Theta^2}$  and combining Eqs. (B3) and (B5) lead to:

$$S = \frac{\mathcal{A}}{2\pi^2} \int_{k_2^{\min}}^{\infty} \frac{k_2 \exp\left(-\beta \frac{\hbar^2 k_2^2}{2m_e}\right) dk_2}{\sqrt{\frac{\hbar^4 k_{\text{cm}}^2 k_2^2}{m_e^2} - \left(E_X - \hbar\Omega - \frac{\hbar^2 k_{\text{cm}}^2}{2m_e}\right)^2}}. \quad (\text{B6})$$

With two successive changes of variables:  $K_2 = k_2^2$  and  $K'_2 = K_2/k_2^{\min 2}$ , Eq. (B6) becomes:

$$S = \frac{\mathcal{A} m_e k_2^{\min}}{4\pi^2 \hbar^2 k_{\text{cm}}} \int_1^{\infty} \frac{\exp\left(-\beta \frac{\hbar^2 k_2^{\min 2}}{2m_e} K'_2\right)}{(K'_2 - 1)^{1/2}} dK'_2. \quad (\text{B7})$$

Considering the identity:  $\int_1^{\infty} e^{-\mu x} (x - 1)^{-1/2} dx = \sqrt{\pi/\mu} e^{-\mu}$ , we find:

$$S = \frac{\mathcal{A} m_e}{4\pi^2 \hbar^2 k_{\text{cm}}} \left(\frac{2\pi m_e}{\beta \hbar^2}\right)^{1/2} \exp\left(-\beta \frac{\hbar^2 k_2^{\min 2}}{2m_e}\right). \quad (\text{B8})$$

Finally, inserting Eq. (B8) into Eq. (B1) and approximating the discrete sum over all the vectors  $\mathbf{k}_{\text{cm}}$  by an integral lead to the following expression of the spontaneous emission rate,  $R_{\text{sp}}^{\text{corr}}(\hbar\Omega)$ , due to the scattering of free electrons with  $1s$  excitons:

$$R_{\text{sp}}^{\text{corr}}(\hbar\Omega) = \frac{F(\Omega)\alpha(1-\alpha)N^2\sqrt{2\pi m_e\beta^3}}{M} \int_0^{\infty} e^{-\beta \left[ \frac{\hbar^2 k_{\text{cm}}^2}{2M} + \frac{m_e}{2\hbar^2 k_{\text{cm}}^2} \left( E_g - E_b^X - \hbar\Omega - \frac{m_h}{m_e} \frac{\hbar^2 k_{\text{cm}}^2}{2M} \right)^2 \right]} |V_{\text{scat}}(k_{\text{cm}})|^2 dk_{\text{cm}}. \quad (\text{B9})$$

---

[1] R. Kubo, J. Phys. Soc. Jpn. **12**, 570 (1957).

[2] P. C. Martin and J. Schwinger, Phys. Rev. **115**, 1342 (1959).

[3] C. H. Henry and R. A. Logan and F. R. Merrit, J. Appl. Phys. **51** (6), 3042 (1980).

[4] S. Schmitt-Rink, C. Ell and H. Haug, Phys. Rev. **B 33**, 1183 (1986).

[5] J. I. Kusano, Y. Segawa, Y. Aoyagi, S. Namba and H. Okamoto, Phys. Rev. B **40**, 1685 (1989).

[6] P. Blood, A. I. Kucharska, J. P. Jacobs, K. Griffiths, J. of Appl. Phys. **70** (3), 1144 (1991).

[7] J. Shah (editor), “Hot carriers in semiconductors nanostuctures: physics and applications”, Academic Press, San Diego (1992).

[8] P. W. M. Blom, P. J. van Hall, C. Smit, J. P. Cuypers, and J. H. Wolter, Phys. Rev. Lett **71**, 3878 (1993).

[9] S. Nüsse, P. Haring Bolivar, H. Kurz, V. Klimov and F. Levy, Phys. Rev. B **56**, 4578 (1997).

[10] M. Kira, F. Jahnke and S. W. Koch, Phys. Rev. Lett. **81**, 3263 (1998).

[11] M. Kira, F. Jahnke, W. Hoyer and S. W. Koch, Prog. Quantum Electron. **23**, 189 (1999).

[12] S. Chatterjee, C. Ell, S. Mosor, G. Khitrova, H. M. Gibbs, W. Hoyer, M. Kira, S. W. Koch, J. P. Prineas and H. Stolz, Phys. Rev. Lett. **92**, 067402 (2004).

[13] J. Szczytko, L. Kappei, J. Berney, F. Morier-Genoud, M. T. Portella-Oberli and B. Deveaud, Phys. Rev. B **71**, 195313 (2005).

[14] C. Benoit à la Guillaume, J. M. Debever and F. Salvan, Phys. Rev. **177**, 567 (1969).

[15] H. Haug and S. W. Koch, Phys. Status Solidi (b) **82**, 531 (1977).

[16] S. W. Koch, H. Haug, G. Schmeider, W. Bohnert and C. Klingshirn, Phys. Status Solidi (b) **89**, 431 (1978).

[17] C. Klingshirn and H. Haug, Phys. Rep. **70**, 315 (1981).

[18] W. Kraeft, K. Killiman and D. Kremp, Phys. Status Solidi (b) **72**, 461 (1975).

[19] R. Zimmermann and H. Stolz, Phys. Status Solidi (b) **131**, 151 (1985).

[20] W. Kraeft, D. Kremp, W. Ebeling and G. Röpke, “Quantum Statistics of Charged Particle Systems”, Plenum, New York (1986).

[21] R. Zimmermann, “Many-particle theory of highly excited semiconductors”, Teubner, Berlin (1988).

[22] M. E. Portnoi and I. Galbraith, Phys. Rev. B **60**, 5570 (1999).

[23] V. V. Nikolaev and M. E. Portnoi, Phys. Status Solidi (a) **190** (1), 113 (2002).

[24] E. Rosenthaler and B. Vinter, “Optoélectronique”, Thomson-CSF and Masson, Paris (1998).

[25] S. W. Koch, “Zur Theorie der Stimulierten Emission in Dichten Exzitonensystemen”, Diploma thesis, J. W. Goethe University, Frankfurt, Germany (1977).

[26] I. Galbraith and S. W. Koch, J. Crystal Growth. **159**,

667 (1996).

[27] M. Combescot and O. Betbeder-Matibet, Phys. Rev. Lett. **93**, 016403 (2004).

[28] Kavokin and G. Malpuech, “Cavity polaritons”, Chapter 4, Elsevier (2003).

[29] F. Calogero, “Variable Phase Approach to Potential Scattering”, Academic Press (1967).

[30] K. Huang, “Statistical Mechanics”, John Wiley & Sons (1987).

[31] F. Stern and W. E. Howard, Phys. Rev. **163**, 816 (1967).

[32] I. S. Gradshteyn and I. M. Ryzhik, “Table of Integrals, Series, and Products”, Academic Press, New York, (1980).

[33] M. Abramovitz and I. A. Stegun, “Handbook of Mathematical Functions”, Dover Publication, New York, (1972).

[34] M. E. Portnoi and I. Galbraith, Phys. Rev. B **58**, 3963 (1998).

[35] H. Haug and S. W. Koch, “Quantum Theory of Electronic and Optical Properties of Semiconductors”, World Scientific Publishing (1993).

[36] C. Ell, R. Blank, S. Benner and H. Haug, J. Opt. Soc. Am. B **6**, 2006 (1989).